Journal of chemical & engineering data

Article

Cite This: J. Chem. Eng. Data 2019, 64, 1063−1071

pubs.acs.org/jced

Equilibrium Adsorption Isotherms for H_2O on Zeolite 13X

Karen N. Son,[†] Tra-My Justine Richardson,[‡] and Gregory E. Cmarik*[,§]

[†]School of Mechanical Engineering, Purdue University, West Lafayette, Indiana 47907, United States

[‡]Logyx LLC, NASA Ames Research Center, Moffett Field, California 94035, United States

[§]Jacobs Space Exploration Group, NASA George C. Marshall Space Flight Center, Huntsville, Alabama 35812, United States

Supporting Information

ABSTRACT: Adsorption isotherms are reported for pure water vapor on zeolite 13X (also called zeolite NaX) pellets. Data were obtained using a gravimetric method over a temperature range of 25 to 100 °C and a pressure range of 0.006 to 25 kPa. These pure-component equilibria are fit with the Sips, Toth, and multisite Langmuir models, all modified with the Aranovich−Donohue (A−D) model. The A−D Sips isotherm is recommended for modeling water adsorption on zeolite 13X because it provides the best agreement with the measured isotherm data.

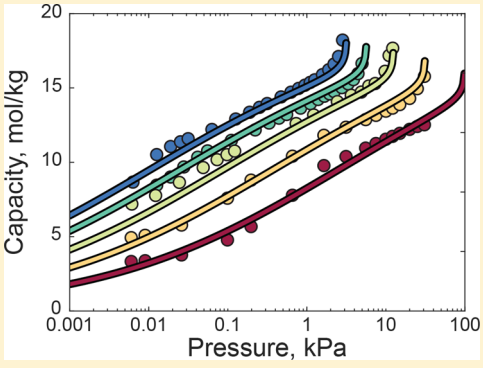

INTRODUCTION

Knowledge of equilibrium adsorption isotherms is critical to the design of adsorption systems; however, accurate isotherms can be challenging to measure even for equilibrium adsorption isotherms of pure gases on commercial adsorbents. One such adsorbate/adsorbent pair that is of great interest is water (H_2O) on zeolite 13X. Zeolite 13X is a commercial name for type X zeolite skeletal structure with Na^+ as the major cation. Zeolite 13X is also commonly referred to as zeolite NaX, molecular sieve 13X, or simply 13X. Many industrial processes (e.g., natural gas purification process[1]) use zeolite 13X to remove water vapor from gas streams. Removing water from gas streams reduces the potential for several undesirable effects, such as hydrate formation, corrosion, and condensation or freezing of moisture.[2] Moisture removal is also an importaint precursor to adsorption of other constituents; one standout example of critical technical interest is the use of adsorbent beds to dehumidify the cabin air of spacecraft prior to carbon dioxide (CO_2) removal.[3,4]

The Carbon Dioxide Removal Assembly (CDRA) is a state-of-the-art CO_2 removal system currently used aboard the International Space Station (ISS). The CDRA operated on fully regenerative thermal-/pressure-swing adsorption process to remove CO_2 from the cabin air. It operates cyclically, employing two desiccant beds and two CO_2 adsorbent beds. As one desiccant bed and one adsorbent bed operate in adsorption mode, the other two beds are desorbing (regenerating).[3] Halfway through a cycle, the beds switch modes, providing continuous CO_2 removal capability for up to six crew members.[5] The National Aeronautics and Space Administration (NASA) is currently redesigning CDRA for use on future crewed space missions.[6] Engineers at NASA are leveraging predictive simulations to optimize the design of a next-generation CO_2 removal system that will use zeolite 13X as both a desiccant and CO_2 adsorbent.[7]

Accurate adsorption equilibrium data of CO_2 and H_2O on zeolite 13X are needed across a wide range of temperatures and pressures to enable these predictive simulations. Though many studies have published data for CO_2 and H_2O adsorption, discrepancies in reported isotherms are common in the literature due to variability in the adsorbents tested and differences in measurement procedures.[8] While in principle the measurement is straightforward and can be accomplished using a variety of commercially available or custom-built instruments, in practice it is challenging to obtain repeatable and accurate measurements. Correct measurements are especially challenging to obtain at low vapor pressures and H_2O loadings, due to finite instrument sensitivities and the difficulty of verifying complete activation of the adsorbent. It is also difficult to determine when equilibrium has been reached in many measurement instruments.

In 2009, Wang and LeVan[9] published several isotherms for CO_2 and H_2O adsorption on zeolite 5A and 13X (Grace Davidson, MS 522 and MS 544 respectively). While the data spanned a wide range of temperatures (0−100 °C) useful for many pressure-swing adsorption (PSA) and temperature-swing adsorption (TSA) applications, their measurements were limited to lower pressures (0.004 to 1.8 kPa). NASA previously used published isotherms, such as those of Wang and LeVan,[9] to model adsorbent-based, atmosphere-revitalization systems (e.g., PSA and TSA). However, the limited pressure range of extant

Received: October 23, 2018
Accepted: January 25, 2019
Published: February 11, 2019

DOI: 10.1021/acs.jced.8b00961
J. Chem. Eng. Data 2019, 64, 1063−1071

data along with unresolved discrepancies between model predictions and experiments required NASA to develop new equilibrium adsorption isotherms for CO_2 and H_2O adsorption on zeolite 13X.[10,11] We presented NASA's equilibrium adsorption isotherms for CO_2 adsorption on zeolite 13X in a prior publication.[11] In that paper,[11] the CO_2/13X isotherms of Wang and LeVan[9] were shown to have an erroneously reduced capacity as a result of the low activation temperature (175 °C) used. This result agreed with the findings of Brandani and Ruthven[12] who documented the effect of temperature on water loading in zeolite 13X. They found that residual water loading remained on 13X adsorbent at temperatures as high as 220 °C; increasing the temperature to 350 °C resulted in complete H_2O removal. H_2O/13X isotherm data from Wang and LeVan is also expected to be biased due to the low activation temperature. Thus, new measurements of water isotherms are needed not only to extend the range of pressure data available but also to correct for possible errors resulting from incomplete activation.

In this paper, we report adsorption isotherms for pure water vapor on commercially available zeolite 13X pellets (Grace Davidson, MS 544). Water isotherms are measured for H_2O adsorption on zeolite 13X; these data are carefully collected to eliminate sources of intrinsic experimental errors in earlier data[9] caused by residual water. We correlate the measured equilibrium data using the Aranovich–Donohue (A–D) model with four different isotherm equations (Sips, Toth, 2-site Langmuir, and 3-site Langmuir). The goodness of fit for each correlation is described in terms of several statistical metrics; this A–D Sips model is recommended for use based on its fit to the experimental data and simplicity.

EXPERIMENTAL METHODS

Isotherms for water adsorption on zeolite 13X are measured at 25 °C, 35 °C, 50 °C, 70 °C, and 100 °C and at equilibrium pressures ranging from 0.006 to 25 kPa. All isotherms were collected at NASA Ames Research Center using a vacuum gravimetric sorption analyzer.

Materials. The adsorbent material used for isotherm is a commercial zeolite 13X (Grace Davison, MS 544). Data were measured for adsorbent pellets from two different lots (no. 216159 and 280254); the variance in capacity between these two lots, as measured via numerous repeat measurements at 25 °C, was found to be less than the sample-to-sample variability of our measurements. The final data reported in this study are taken from the most recently produced batch of adsorbent (lot no. 280254) with the exception of the 35 °C isotherm which was only measured for lot no. 216159. The adsorbent is characterized in the manufactured form as pelletized, spherical beads with a mean diameter of 2 mm which contain 18% binder on a dry weight basis. While adding binder is necessary to structure the zeolite crystals into pellets that allow a reasonable pressure drop across the bed, binder can negatively impact the capacity of the adsorbent material. While this is mostly due to the addition of nonactive mass, more complex interactions with binder material blocking pore access into the zeolite crystals can also occur.[13] Deionized water (Millipore Milli-Academic, 18.2 MΩ) is used as the adsorbate. Note that zeolite 13X is extensively used in current NASA systems for life support and that MS 544 is the primary zeolite 13X candidate for next-generation adsorbent-based, life-support systems.[14]

Sample Preparation and Activation. The zeolite 13X adsorbent is carefully activated prior to measuring the equilibrium adsorption capacity to ensure complete removal of water and other adsorbed constituents. First, ~30 mg of adsorbent (4–5 beads) is placed into the sample pan. The zeolite 13X is activated by heating the sample in situ with the internal preheater to 350 °C (at 1.8 °C/min) and holding it at this temperature under vacuum (<0.01 mTorr) for 4 h. This high activation temperature is necessary to remove all residual water from the adsorbent pores; lower activation temperatures (≤300 °C) were found to provide inconsistent results that were attributed to incomplete desorption of water affecting the measured capacity of other sorbates.[11,15] After the sample activation is complete, the sample is slowly cooled under vacuum to the desired temperature for isotherm measurements.

Measurement Procedure. An automated gravimetric method is used to measure loading at a single temperature (isotherm) across a range of water vapor pressures. These isotherms are measured in a vacuum gravimetric sorption analyzer (Surface Measurement Systems, DVS Vacuum).[16] This instrument is comprised of a microbalance in a vacuum chamber that holds the adsorbent sample, a flask of liquid water, and flow controls to provide adsorbate gas to the sample, instrumentation, vacuum pumps, and a thermal chamber (see Figure 1). The

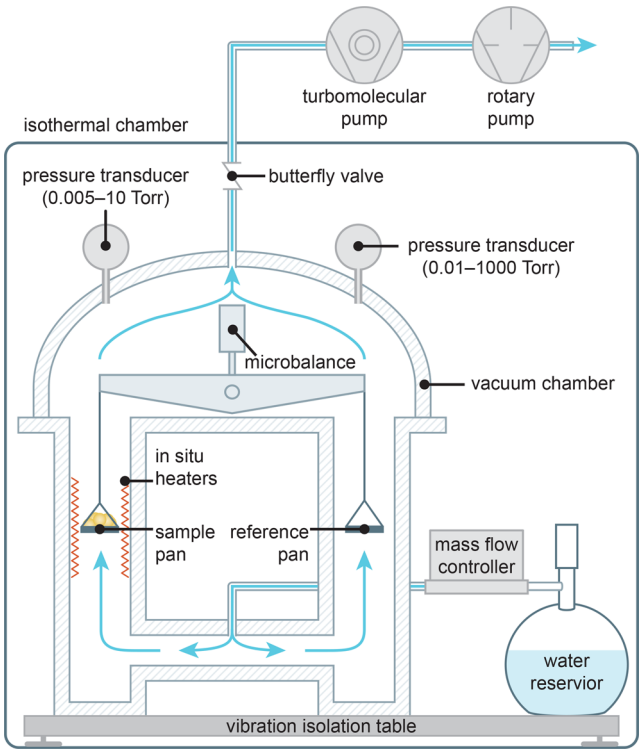

Figure 1. Schematic diagram of the Vacuum Dynamic Vapor Sorption (Surface Measurement Systems, DVS Vacuum) instrument[16] used to measure H_2O adsorption isotherms on zeolite 13X pellets.

thermal chamber houses most of these components, including the vacuum chamber and water flask, and sets the temperature of both the vapor-generation system and the adsorbent sample to within 0.1 °C. The thermal chamber serves to both prevent condensation and to provide a stable, accurate environment for measurement. Isotherm measurements are made using the dynamic measurement mode[16] of the DVS Vacuum sorption analyzer. In this mode, a continuous flow of water vapor is provided to the vacuum chamber throughout adsorption while constant pressure is maintained via a butterfly valve that meters the vacuum conductance. The DSV Vacuum sorption analyzer

DOI: 10.1021/acs.jced.8b00961
J. Chem. Eng. Data 2019, 64, 1063–1071

can measure isotherms in a temperature range of 20−70 °C within a relative humidity range 0.05−90% RH. Higher temperature isotherms can be measured but only under a reduced relative humidity range. This is due to the maximum temperature of the thermal control chamber (70 °C) which limits the source water vapor pressure to approximately 28.2 kPa (i.e., 90% of the saturated vapor pressure of water at 70 °C). The 100 °C isotherm is obtained using the preheater to maintain the adsorbent at 100 °C while the ambient chamber is held at 70 °C. This is the same preheater used during activation which can control the temperature of the sample chamber to within ±1.0 °C.

To generate a desired water vapor concentration, water vapor inside the side arm flask flows through a mass flow controller (Figure 1). The flask contains a two-phase mixture of liquid and vapor water at thermodynamic equilibrium with the temperature of the thermal chamber. Water vapor flow from the flask is induced by a low pressure in the vacuum chamber which pulls the vapor through the side arm flask and up over the sample. Two vacuum pumps and a butterfly valve in series maintain this constant, subambient pressure in the vacuum manifold while the water vapor flow rate is independently controlled via a flow controller throughout adsorption. The butterfly valve maintains the desired pressure inside the vacuum chamber by adjusting the opening size in a feedback loop with the pressure transducers while changes in sample mass are simultaneously measured (Surface Measurement Systems, Ultrabalance, 1−1000 mg full-scale range, 0.1 μg precision). This setup allows for water vapor pressures within the vacuum chamber to reach approximately 90% of the saturated vapor pressure of the flask (i.e., the saturated vapor pressure at the thermal chamber's temperature). Two pressure transducers (MKS Instruments, Baratron transducers, 0.01−1000 Torr and 0.005−10 Torr full-scale ranges, 0.5% reading accuracy, 0.01% FS resolution) continuously measure the pressure inside the vacuum chamber. The water vapor pressure is held constant until the adsorbent reaches equilibrium with the gas stream ($dm/dt < 0.006\%/min$).

Further measurements are taken at successively higher concentrations of water vapor obtained by increasing the pressure within the chamber while maintaining the same total flow rate. This process of increasing the H_2O concentration, equilibrating the sample, and recording the change in mass is repeated to obtain the equilibrium concentration of H_2O at many partial pressures for a single isotherm. This entire process was repeated to obtain isotherms at five different temperatures between 25 and 100 °C.

Isotherm Models. Per the International Union of Pure and Applied Chemistry (IUPAC) classification of gas−solid adsorption isotherms,[17] the experimental isotherms obtained are of type II because they exhibit a sigmoidal shape with an apparent divergence of n to infinity as the water vapor partial pressure, p, approaches the water-vapor saturation pressure, p_{sat}. Type II isotherms are observed for materials with a range of pore sizes; there is initially monolayer adsorption within the microporous solid at lower H_2O partial pressures, followed by multilayer adsorption and then capillary condensation.[18,19] The divergence of capacity at high p/p_{sat} values is caused by capillary condensation occurring in pores of increasing diameter[19] (e.g., the macropores formed by the clay binder in the zeolite pellets[20]). Aranovich and Donohue[21] proposed the following model to account for the singularity at $p = p_{sat}$

$$n = \frac{f(p, T)}{\left(1 - \frac{p}{p_{sat}}\right)^d} \tag{1}$$

where n is the equilibrium adsorbed-phase concentration, T is the temperature of the adsorbent (e.g., zeolite 13X), where $f(p)$ is a function describing the adsorption of the first molecular layer, d is an adjustable parameter, and p_{sat} is the saturation-vapor pressure as calculated by the Antoine equation[22]

$$p_{sat}(T) = 100 \times 10^{4.6543 - (1435.264/T - 64.848)} \tag{2}$$

The function $f(p,T)$ can be expressed using several equilibrium adsorption isotherm models. In the present work, we consider four isotherm models for $f(p,T)$, including the Sips model[23]

$$f(p, T) = \frac{a(bp)^{1/h}}{1 + (bp)^{1/h}} \tag{3}$$

Toth model[24]

$$f(p, T) = \frac{abp}{[1 + (bp)^h]^{1/h}} \tag{4}$$

and multisite (i.e., k-site) Langmuir model[25,26]

$$f(p, T) = \sum_{j=1}^{k} \frac{a_j b_j p}{1 + b_j p} \tag{5}$$

where a_0 is the saturation capacity, b is the temperature-dependent equilibrium constant

$$b_j = b_{0,j} \exp\left[\frac{E_j}{(RT_s)}\right] \tag{6}$$

and h describes the surface heterogeneity. The parameters a, b_0, E, h, and d are system-dependent, adsorption-isotherm parameters which we fit to the experimental data.

Fitting Method. We follow the method described in Son et al.[11] to fit the isotherm models to experimental data. This method uses a custom implementation of the generalized reduced gradient (GRG) nonlinear solver in Excel to find the parameters which minimized the sum of squares error, SSE, defined as

$$\mathrm{SSE} = \sum (n_{pred} - n_{meas})^2 \tag{7}$$

where n_{meas} is the measured amount adsorbed and n_{pred} is the predicted amount adsorbed based on the isotherm model and fit parameters. The *SSE* is found by summing over all experimental measurements; thus, regions of data with higher pressures and lower temperatures having larger absolute values of n_{meas} and n_{pred} will lead to higher absolute differences and will be emphasized more in the resulting fit. The GRG nonlinear solver converges to a residual of 1×10^{-12}. To improve convergence and prevent ill-conditioning, the parameters actively modified by the solver are normalized to be of the same order of magnitude every 1000 iterations. This is done by dividing the actual model fit parameters by their order of magnitude to obtain a value of ∼1.

RESULTS AND DISCUSSION

Isotherms for water adsorption on zeolite 13X (Grace Davidson, MS 544) were measured at 25 °C, 35 °C, 50 °C, 70 °C, and 100

DOI: 10.1021/acs.jced.8b00961
J. Chem. Eng. Data 2019, 64, 1063−1071

Table 1. Adsorption Equilibria of H_2O on Zeolite 13X (25 °C, 35 °C, 50 °C, 70 °C, and 100 °C)

25 °C		35 °C		50 °C		70 °C		100 °C	
p kPa	*n* mol/kg	*p* kPa	*n* mol/kg	*p* kPa	*n* mol/kg	*p* kPa	*n* mol/kg	*p* kPa	*n* mol/kg
0.0064	8.6 ± 0.9	0.0128	8.4 ± 0.9	0.0062	7.1 ± 0.7	0.0061	4.9 ± 0.5	0.0061	3.3 ± 0.4
0.0128	10.5 ± 1.1	0.0192	9.0 ± 0.9	0.0124	7.7 ± 0.8	0.0091	5 ± 0.5	0.0091	3.3 ± 0.4
0.0192	11.0 ± 1.1	0.0281	9.6 ± 1.0	0.0247	8.6 ± 0.9	0.0263	5.7 ± 0.6	0.0263	3.7 ± 0.4
0.0256	11.3 ± 1.2	0.0422	10.3 ± 1.1	0.0495	9.6 ± 1	0.100	7.5 ± 0.8	0.100	4.7 ± 0.5
0.0319	11.5 ± 1.2	0.0563	10.7 ± 1.1	0.0742	10.1 ± 1	0.200	8.7 ± 0.9	0.200	5.6 ± 0.6
0.0639	12.1 ± 1.2	0.1125	11.4 ± 1.2	0.0990	10.5 ± 1.1	0.667	10.3 ± 1.1	0.667	7.7 ± 0.8
0.128	12.8 ± 1.3	0.225	12.1 ± 1.2	0.124	10.7 ± 1.1	1.67	11.8 ± 1.2	1.667	9.7 ± 1
0.192	13.3 ± 1.3	0.338	12.6 ± 1.3	0.742	12.5 ± 1.3	3.17	12.3 ± 1.3	3.173	10.3 ± 1.1
0.255	13.6 ± 1.4	0.450	12.9 ± 1.3	1.237	13.1 ± 1.3	5.63	12.8 ± 1.3	5.627	10.9 ± 1.1
0.319	13.9 ± 1.4	0.563	13.2 ± 1.3	2.466	14 ± 1.4	7.60	13.1 ± 1.3	7.599	11.2 ± 1.1
0.479	14.3 ± 1.4	0.844	13.6 ± 1.4	3.700	14.4 ± 1.5	10.1	13.4 ± 1.4	10.132	11.5 ± 1.2
0.639	14.7 ± 1.5	1.125	13.9 ± 1.4	4.949	14.7 ± 1.5	12.3	13.6 ± 1.4	12.332	11.7 ± 1.2
0.798	14.9 ± 1.5	1.407	14.2 ± 1.4	6.166	15.1 ± 1.5	15.2	13.8 ± 1.4	15.199	11.9 ± 1.2
0.958	15.1 ± 1.5	1.688	14.4 ± 1.5	7.423	15.2 ± 1.5	20.3	14.2 ± 1.4	20.265	12.2 ± 1.2
1.12	15.3 ± 1.5	1.97	14.5 ± 1.5	9.90	16.1 ± 1.6	25.33	14.9 ± 1.5	25.33	12.4 ± 1.3
1.28	15.5 ± 1.6	2.25	14.7 ± 1.5	11.14	17.1 ± 1.7				
1.60	15.8 ± 1.6	2.81	15.0 ± 1.5	12.37	17.6 ± 1.8				
1.92	16.2 ± 1.6	3.38	15.2 ± 1.5						
2.24	16.5 ± 1.7	3.94	15.5 ± 1.6						
2.55	17.1 ± 1.7	4.50	15.9 ± 1.6						
2.87	18.2 ± 1.8	5.06	16.6 ± 1.7						

Table 2. Summary of the Water Vapor Isotherms Collected from the Literature[a]

authors	year	adsorbent description	binder	activation	measurement technique	*T*, °C
Chuikina et al.[29]	1976	lab-made[c]	–	400 °C for 100 h (unspecified atmosphere)	calorimetric-volumetric	23, 100
Gopal et al.[30]	1982	Linde powder[c]	–	300 °C in ambient air for 24 h	N/A	25
Zhu et al.[31]	1992	lab-made pellets[c]	15%[b]	N/A	N/A	40, 60, 80, 100
Ryu et al.[27]	2001	Aldrich pellets	20%[b]	340 °C for 7 h (unspecified atmosphere)	gravimetric	25, 35, 45
Kim et al.[28]	2003	Aldrich pellets	20%[b]	320 °C in vacuum (10^{-3} Pa) for 24 h	volumetric (ASAP 2010, Micromeritics)	20, 40, 60, 80
Ahn and Lee[19]	2004	Aldrich pellets	20%[b]	320 °C for 12 h (unspecified atmosphere)	N/A	25, 35, 45
Li et al.[32]	2009	MOLSIV, UOP[c]	20%[b]	320 °C (unspecified atmosphere and *t*)	gravimetric (IGA-002, Hiden Isochema, Ltd.)	25
Wang and LeVan[9]	2009	MS 544, Grace Davidson	18%	175 °C in vacuum overnight	volumetric	0–100
Ferreira et al.[33]	2011	ZEOX OII pellets, Zeochem	20%[b]	375 °C in N_2 atmosphere for 6 h	gravimetric (Rubotherm)	35
		Z10–02ND pellets, Zeochem[c]	20%[b]	375 °C in N_2 atmosphere for 6 h	gravimetric (Rubotherm)	35
Chen et al.[34]	2012	Nanjing Inorganic Chemical Plant[c]	–	450 °C for 2 h (unspecified atmosphere)	vacuum-gravimetric	25
Hefti et al.[35]	2014	ZeoChem[c]	20%	400 °C in vacuum for 4 h	gravimetric	45
Mette et al.[36]	2014	13XBFK, Chemiewerk[c]	–	350 °C in vacuum, < 10^{-5} mbar (unspecified *t*)	gravimetric (IGA-002, Hiden Isochema, Ltd.)	25–250
Kim et al.[2]	2016	APG MOLSIV, UOP[c]	20%	300 °C in vacuum for 12 h	volumetric (ASIQM0 V000-4, Quantachrome)	20, 30, 40
Lehmann et al.[37]	2017	13XBFK, Chemiewerk[c]	–	400 °C in vacuum, < 0.05 Pa, for 16 h	gravimetric (IGA-002, Hiden Isochema, Ltd.)	31–250
Semprini et al.[38]	2017	13XBFK, Chemiewerk[c]	–	350 °C in vacuum, < 10^{-5} mbar (unspecified *t*)	gravimetric (IGA-002, Hiden Isochema, Ltd.)	25–250

[a]A dash (–) in the binder column indicates pure crystalline samples were used (i.e., no binder). [b]Estimated binder mass fraction. [c]Adsorbents that exhibited a higher capacity.

°C and at equilibrium pressures ranging from 0.006 to 25 kPa or from relative humidities of 0.05–90%. The experimental adsorption equilibrium data are presented in Table 1. The uncertainty in the pressure reading is ±0.5% of the measured pressure. All experimental values were measured in duplicate with resulting repeatability within 10%; this is taken as the uncertainty in the final measured loading *n*. The experimental adsorption equilibrium data obtained in the present work are compared with H_2O/13X adsorption data from the literature. The present data are then correlated with the Aranovich–Donohue (A–D) Sips, Toth, and multisite Langmuir models.

DOI: 10.1021/acs.jced.8b00961
J. Chem. Eng. Data 2019, 64, 1063–1071

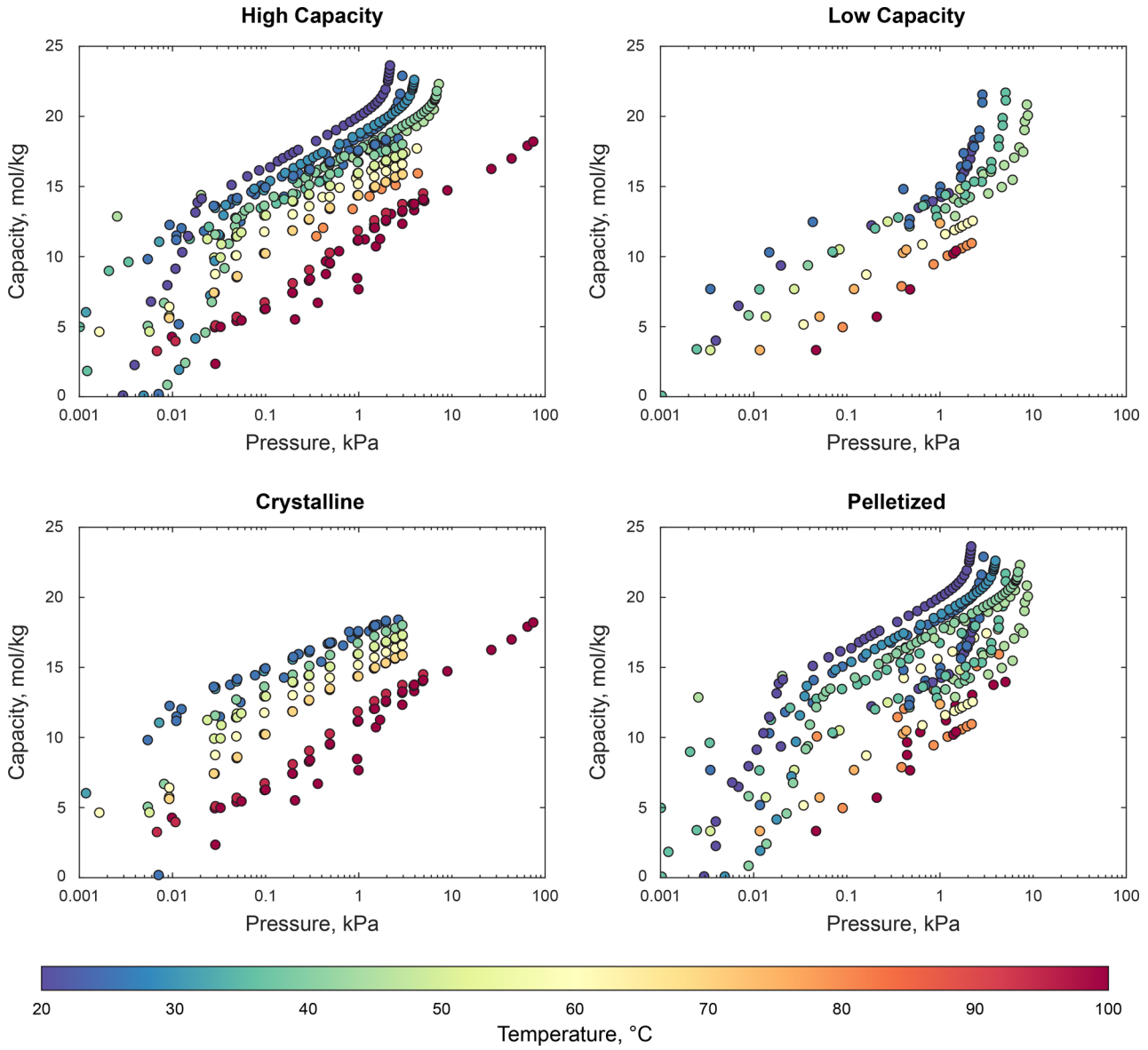

Figure 2. Water on zeolite 13X isotherms from the literature.[2,9,19,27−38] The isotherms are grouped based on the adsorbent's capacity (top panels); most of the isotherms[2,29−38] exhibit a high capacity for water (left), while a few[9,19,27,28,33] isotherms show a lower capacity (right). Isotherms are also grouped by adsorbent type (bottom panels), being either crystalline[29,30,34,36−38] (left) or pelletized[2,9,19,27,28,31−33,35] (right).

The resulting goodness of fits are then compared between models and recommendations are made for which model to use.

Comparison of Isotherm Data to the Literature. Experimental data for water isotherms on zeolite 13X are collected from the literature along with details on the adsorbent, activation procedure, and measurement technique where available. Table 2 summarizes the adsorption isotherms extracted from the literature;[2,9,19,27−38] studies with isotherms which were found to be inconsistent either in shape (e.g., crossing isotherms or negative slopes) or magnitude (i.e., loading >50% discrepancy from the cluster of other isotherms) are excluded from this list. To allow for direct comparison between pure, crystalline samples and pelletized adsorbents, we normalize the reported loading as

$$n^* = \frac{n}{1 - (\text{binder mass fraction})} \quad (8)$$

Where a study does not explicitly state the binder's mass fraction, the binder mass fraction must be assumed. The commercial adsorbents used in Ryu et al.,[27] Kim et al.,[28] Ahn and Lee,[19] Li et al.,[32] and Ferreira et al.[33] are estimated to contain 20% binder by mass to make their measured loadings consistent with studies of crystalline 13X or pellets with a known binder mass fraction. The lab-made adsorbent in Zhu et al.[31] is estimated to contain 15% binder mass fraction following the same approach. This is the same method for estimating binder mass fraction used by Loughlin et al.[39] in their review of isotherms for multiatomic species on zeolites. The binder content of Grace Davidson MS 544, the adsorbent used both by Wang and LeVan[9] and in the present study, was previously found to be 18%.[11] All data plotted in Figures 2−4 are normalized using eq 8 and the binder mass fractions listed in Table 2.

The studies listed in Table 2 can be divided into two groups based on their capacity for H_2O adsorption. Most of the

DOI: 10.1021/acs.jced.8b00961
J. Chem. Eng. Data 2019, 64, 1063−1071

studies[2,29−38] showed a similar, high capacity of approximately 18.5 mol/kg at 1 kPa of water vapor and 25 °C. These high-capacity isotherms are plotted in the upper left panel of Figure 2 and are highlighted in green in Table 2. Isotherms from remaining five studies,[9,19,27,28,33] which show a significantly lower capacity of ∼15 mol/kg at 1 kPa of water vapor and 25 °C, are plotted in the upper right panel of Figure 2. Ferreira et al.[33] measured isotherms for two different commercial 13X samples, Z10-02ND, and ZEOX O_{II} (Zeochem). The first adsorbent, Z10-02ND, exhibited high water capacity and is plotted in the upper left panel of Figure 2 while the second adsorbent, ZEOX O_{II}, is grouped with the low-capacity isotherms in the upper right panel. We attribute this difference in capacity for these two Zeochem adsorbents to differences in their formulations. All three studies on Aldrich pellets[19,27,28] consistently exhibited low-capacity isotherms compared to the bulk of isotherms from the literature, indicating a difference in pellet formulation which yields capacity similar to ZEOX O_{II}. We attribute the low-capacity isotherms from the final study[9] to incomplete activation caused by inadequate activation temperature.

Through extensive comparison of CO_2 isotherms on zeolite 13X from four separate research facilities (NASA Marshall, NASA Ames, University of South Carolina, and Vanderbilt University) NASA found that activation at lower temperatures (e.g., 300 °C) caused incomplete desorption of water and resulted in discrepancies between different isotherm measurements.[15,40] All discrepancies between the different research facilities and measurement techniques (e.g., gravimetric versus volumetric) were resolved by using an activation temperature of 350 °C. NASA's results confirm the findings of Brandani and Ruthven[12] who found that zeolite 13X needed to be activated at 350 °C to completely remove H_2O. In their study, Wang and LeVan[9] used the same adsorbent (Grace Davidson, MS 544) as the present work, however, they used a much lower activation temperature (175 °C). Based on our previous findings, we expected that these H_2O/13X isotherm data would be biased due to residual water loading. This theory is confirmed by comparing the 25 °C, 50 °C, 75 °C, and 100 °C isotherms of Wang and LeVan[9] to the current data (see Figure 3). Note that Wang and LeVan's isotherm at 75 °C is slightly hotter than the 70 °C isotherm data from the present work. The values reported by Wang and LeVan[9] are consistently lower by 1 mol/kg to 2 mol/kg with the largest discrepancies seen in the lowest temperature isotherms and in the low-pressure region. These results clearly show that a high activation temperature (e.g., 350 °C) is required to obtain accurate water isotherm data.

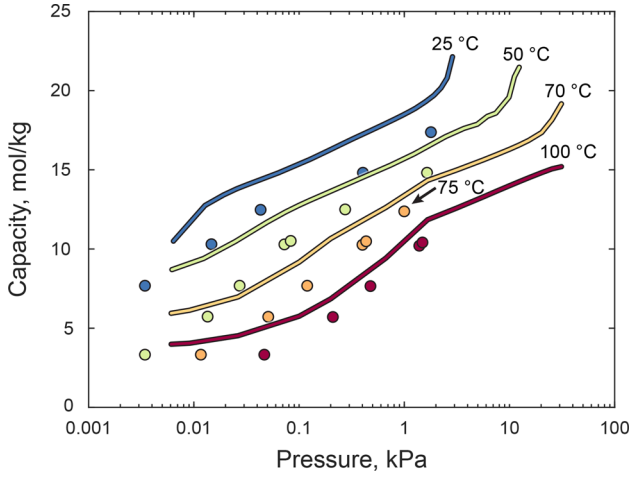

Figure 3. Comparison of isotherms for H_2O on zeolite 13X from current work (lines) to values from Wang and LeVan[9] (circles).

In addition to grouping isotherms based on capacity, isotherms from the literature can be grouped based on the type of adsorbent used in their measurements (i.e., pelletized or crystalline) as shown in the bottom panels of Figure 2. Isotherms measured on pelletized adsorbents[2,9,19,27,28,31−33,35] (right) showed different behavior than those measured on pure crystals[29,30,34,36−38] (left) at high pressures. In pelletized adsorbents, the loading rapidly increases as the water vapor partial pressure approaches the saturation pressure, causing condensation within the mesopores and macropores of the pellets.[19] Because the isotherms obtained from the crystalline adsorbents do not extend into the region where the effects of binder are evident (i.e., high pressures where macropore condensation occurs[41]), they can be directly compared with isotherms from pelletized adsorbents. As such, we retain data for crystalline adsorbents when comparing our measurements to isotherms from the literature.

A comparison of the current isotherm results for water adsorption on zeolite 13X to data from the literature[2,29−38] is presented in Figure 4, which shows the equilibrium capacity of zeolite 13X as a function of H_2O pressure. Isotherm data measured on Aldrich[19,27,28] and Zeochem ZEOX O_{II}[33] adsorbents are excluded due to differences in the zeolite formulations. The data of Wang and LeVan[9] are also excluded due to the low activation temperature which was insufficient to remove residual water loading. Our data match both the slope and general magnitude of the literature data. We note that there is some scatter among the isotherms from the literature which we attribute to differences in the adsorbents tested. This scatter emphasizes the importance of measuring isotherm data for the specific adsorbent formulation of interest to achieve maximum accuracy. Water and carbon dioxide[11] adsorption on Grace Davidson MS 544 is of particular interest as MS 544 was recently

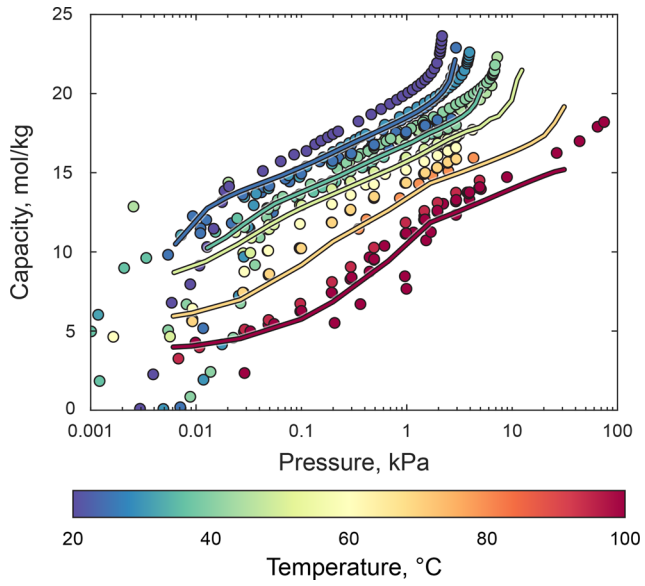

Figure 4. Comparison of isotherms for H_2O on zeolite 13X from current work (lines) to values from the literature.[2,29−38]

DOI: 10.1021/acs.jced.8b00961
J. Chem. Eng. Data 2019, 64, 1063−1071

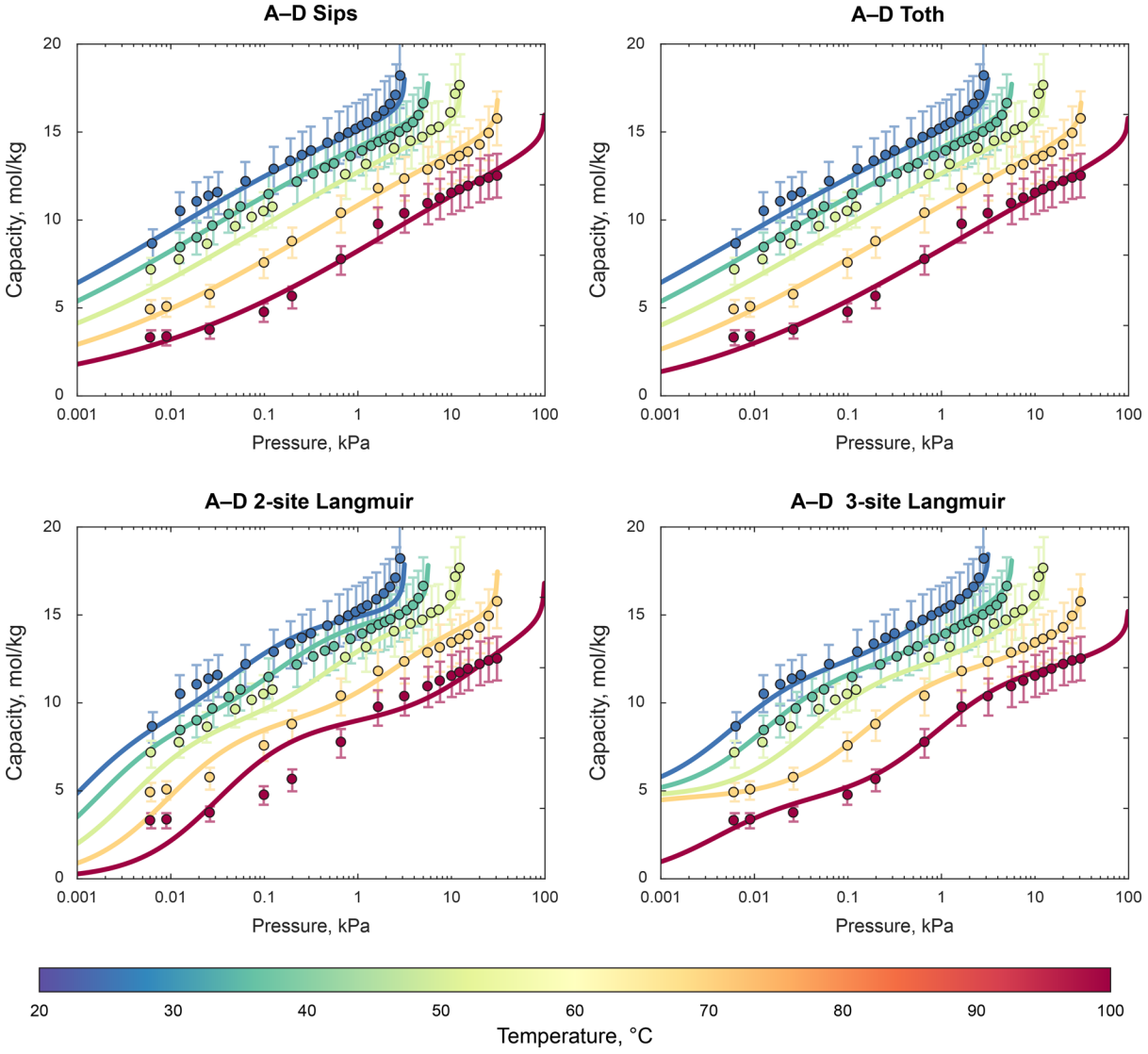

Figure 5. Measured isotherms from the current work (symbols) for H_2O adsorption on zeolite 13X compared to isotherm model predictions (lines).

selected for use in NASA's next-generation life-support systems.[14]

Comparison of Isotherm Data to Fitted Models. The isotherm models given in eq 4 through eq 5 are fit to our experimental data as described in Fitting Method section above with the resulting fits shown in Figure 5. The accuracy of each model fit to the experimental data is quantified using the root-mean-square error (RMSE), the normalized-root-mean-square error (NRMSE), the maximum error (E_{max}), the normalized-maximum error (NE_{max}), and the regression coefficient (R^2) as given in Table 3. The Aranovich–Donohue (A–D) 2-site Langmuir model predictions deviate from the experimental measurements as shown in Figure 5, with the model predictions falling outside of the 95% confidence interval of measured loading values at low vapor pressures for the 40 and 100 °C isotherms. The A–D 2-site Langmuir model also yields the worst values for each goodness-of-fit metric considered in Table 3. Comparing the remaining three models requires a closer look at the plotted comparisons in combination with the values in Table 3. For example, while the A–D 3-site Langmuir model appears to provide an excellent fit based on the RMSE and R^2 values (0.404 mol/kg and 0.985, respectively), the plotted model predictions show nonphysical artifacts. Most notably, the predicted isotherms diverge from the theoretically expected Henry's law behavior at low vapor pressures.[18] Not only are these inflections thermodynamically inconsistent with H_2O adsorption on zeolite 13X, but they can also result in significant model errors if the Clausius–Clapeyron equation is used to predict the heat of adsorption.[11] These spurious fitting artifacts are caused by a larger number of free parameters (i.e., overfitting). The A–D Sips model also fits the data very well (RMSE = 0.472 mol/kg, R^2 = 0.979) but has half the number of

Table 3. Comparison of the Goodness of Fit for the Different Isotherm Models

model	no. of fit parameters	RMSE, mol/kg	NRMSE	E_{max}, mol/kg	NE_{max}	R^2
A–D Sips	5	0.472	0.0492	1.31	0.149	0.979
A–D Toth	5	0.463	0.0497	1.21	0.151	0.979
A–D 2-site Langmuir	7	0.612	0.0616	1.88	0.260	0.965
A–D 3-site Langmuir	10	0.404	0.0411	1.47	0.206	0.985

DOI: 10.1021/acs.jced.8b00961
J. Chem. Eng. Data 2019, 64, 1063–1071

fitted parameters, which significantly reduces the risk of overfitting.

The RMSE, max error, and R^2 values do not provide a complete picture of the goodness of fit at low loadings because they are absolute measures of the error. Two additional relative error metrics are therefore considered to better quantify the goodness of fit at low loadings: the NE_{max} and the NRMSE

$$\mathrm{NRMSE} = \sqrt{\frac{1}{k}\sum_{i=1}^{k}\left(\frac{(n_{pred} - n_{meas})^2}{n_{meas}}\right)} \quad (9)$$

These normalized metrics highlight the risks associated with overfitting data. Note that the multisite Langmuir models have almost double the normalized-maximum error as the much simpler Sips or Toth models. The normalized metrics also show that the A−D Sips model (NRMSE = 0.0492 and NE_{max} = 0.149) provides a slightly better fit than the A−D Toth model (NRMSE = 0.0497 and NE_{max} = 0.151). Based on these goodness-of-fit parameters, we recommend using the A−D Sips isotherm model as given by eqs 1−3 with the fitted parameters listed in Table 4. Fit parameters for the other models considered in this paper are provided in Supporting Information. The isotherms are only recommended for use within the bounds of the experimental measurements (i.e., 0.006 to 25 kPa and 20 to 100 °C) and for zeolite 13X with similar formulation to the tested adsorbent.

Table 4. Fit Parameters for the A−D Sips Isotherm Model for H_2O Adsorption on Zeolite 13X (Grace Davidson, MS 544)

a_0, mol/kg	b_0, kPa^{-1}	E/R, K	f_0	d
18.87	1.353×10^{-10}	8150	0.288	0.02772

CONCLUSIONS

Accurate isotherm fits are a critical component of predictive adsorption models; good isotherm fits depend on both precise measurements and appropriate selection of the equilibrium adsorption isotherm equation. Isotherms for H_2O adsorption on commercially available zeolite 13X (Grace Davidson MS 544) are measured at five temperatures from 25 to 100 °C and at pressures from 0.006 to 25 kPa. Our measurements compare favorably to other isotherm measurements in the literature and show the importance of careful collection techniques. We specifically showed that a high activation temperature (350 °C) is needed to obtain accurate water isotherms by comparing against experimental results from the literature which showed a reduced capacity due to incomplete removal of water at a lower activation temperature (175 °C). We then fit the Sips, Toth, 2-site Langmuir, and 3-site Langmuir (all modified with the Aranovich−Donohue equation) to our experimental measurements to determine the isotherm model that offers the best representation of the measured data. From this comparison, we recommend using the A−D Sips isotherm model as given by eqs 1−3 with the fitted parameters listed in Table 4 when modeling water adsorption on zeolite 13X. While the isotherm fit presented in this work was developed for modeling life-support systems, it can be broadly used in the design of numerous other adsorption systems such as gas stream dehumidification, industrial processes, and natural gas purification process.

ASSOCIATED CONTENT

Supporting Information

The Supporting Information is available free of charge on the ACS Publications website at DOI: 10.1021/acs.jced.8b00961.

Fit parameters for the all models considered in this paper other than the A−D Sips are listed in Tables S1−S3(PDF)

AUTHOR INFORMATION

Corresponding Author

*E-mail: gregory.e.cmarik@nasa.gov.

ORCID

Karen N. Son: 0000-0003-0910-356X

Notes

The authors declare no competing financial interest.

ACKNOWLEDGMENTS

We thank Dr. Vladimir Martis of Surface Measurement Systems U.K. Ltd. for his assistance in developing the isotherm measurement procedures and in ensuring the accuracy of this paper.

REFERENCES

(1) Shirani, B.; Kaghazchi, T.; Beheshti, M. Water and Mercaptan Adsorption on 13X Zeolite in Natural Gas Purification Process. *Korean J. Chem. Eng.* **2010**, *27*, 253−260.

(2) Kim, K.-M.; Oh, H.-T.; Lim, S.-J.; Ho, K.; Park, Y.; Lee, C.-H. Adsorption Equilibria of Water Vapor on Zeolite 3A, Zeolite 13X, and Dealuminated Y Zeolite. *J. Chem. Eng. Data* **2016**, *61*, 1547−1554.

(3) Kay, R. International Space Station (ISS) Carbon Dioxide Removal Assembly (CDRA) Protoflight Performance Testing, 28th International Conference on Environmental Systems, Danvers, MA, July 13−16, 1998.

(4) Hopson, G. D. L. *Skylab Environmental Control and Life Support Systems*; American Society of Mechanical Engineers: San Francisco, CA, 1971; pp 71-AV-14.

(5) Knox, J. C. International Space Station Carbon Dioxide Removal Assembly Testing, 30th International Conference on Environmental Systems, Toulouse, France, July 10−13, 2000.

(6) Knox, J. Development of Carbon Dioxide Removal Systems for NASA's Deep Space Human Exploration Missions 2017−2018, 48th International Conference on Environmental Systems, Albuquerque, NM, July 8−12, 2018.

(7) Giesy, T. J. C. CO_2 Virtual Design of a 4-Bed Molecular Sieve for Exploration, 47th International Conference on Environmental Systems, Charleston, SC, July 16−20, 2017.

(8) Dirar, Q. H.; Loughlin, K. F. Intrinsic Adsorption Properties of CO2 on 5A and 13X Zeolite. *Adsorption* **2013**, *19*, 1149−1163.

(9) Wang, Y.; LeVan, M. D. Adsorption Equilibrium of Carbon Dioxide and Water Vapor on Zeolites 5A and 13X and Silica Gel: Pure Components. *J. Chem. Eng. Data* **2009**, *54*, 2839−2844.

(10) Huang, R.; Belancik, G.; Jan, D.; Knox, J. C.; Richardson, T.-M. J. CO_2 Capacity Sorbent Analysis Using Volumetric Measurement Approach. 47th International Conference on Environmental Systems; Charleston, SC, July 16−20, 2017.

(11) Son, K. N.; Cmarik, G. E.; Knox, J. C.; Weibel, J. A.; Garimella, S. V. Measurement and Prediction of the Heat of Adsorption and Equilibrium Concentration of CO2 on Zeolite 13X. *J. Chem. Eng. Data* **2018**, *63*, 1663−1674.

(12) Brandani, F.; Ruthven, D. M. The Effect of Water on the Adsorption of CO2 and C3H8 on Type X Zeolites. *Ind. Eng. Chem. Res.* **2004**, *43*, 8339−8344.

(13) Whiting, G.; Chowdhury, A.; Oord, R.; Paalanen, P.; Weckhuysen, M. The Curious Case of Zeolite−Clay/Binder

DOI: 10.1021/acs.jced.8b00961
J. Chem. Eng. Data 2019, 64, 1063−1071

Interactions and Their Consequences for Catalyst Preparation. *Faraday Discuss.* **2016**, *188*, 369−386.
(14) Knox, J.; Cmarik, G.; Watson, D.; Miller, L.; Giesy, T. Investigation of Desiccants and CO_2 Sorbents for Exploration Systems 2016−2017, 47th International Conference on Environmental Systems, Charleston, SC, July 16−20, 2017.
(15) Erden, L.; Ebner, A. D.; Nicholson, M. A.; Holland, C. E.; Ritter, J. A.; Trinh, D.; Shapiro, A.; Knox, J. C.; Mitchell, L. A.; LeVan, M. D. On the Variability and Reproducibility of Equilibrium Adsorption Isotherm Measurements from Different Laboratories, AIChE Annual Meeting, San Francisco, CA, November 3−8, 2013.
(16) *Dynamic Dual Vapor/Gas Gravimetric Sorption Analyzer Product Brochure*; Surface Measurement Systems, 2015.
(17) Rouquerol, J.; Avnir, D.; Fairbridge, C. W.; Everett, D. H.; Haynes, J. M.; Pernicone, N.; Ramsay, J. D. F.; Sing, K. S. W.; Unger, K. K. Recommendations for the Characterization of Porous Solids (Technical Report). *Pure Appl. Chem.* **1994**, *66*, 1739−1758.
(18) Ruthven, D. M. *Principles of Adsorption and Adsorption Processes*; John Wiley & Sons: New York, 1984.
(19) Ahn, H.; Lee, C.-H. Effects of Capillary Condensation on Adsorption and Thermal Desorption Dynamics of Water in Zeolite 13X and Layered Beds. *Chem. Eng. Sci.* **2004**, *59*, 2727−2743.
(20) Schumann, K.; Unger, B.; Brandt, A.; Scheffler, F. Investigation on the Pore Structure of Binderless Zeolite 13× Shapes. *Microporous Mesoporous Mater.* **2012**, *154*, 119−123.
(21) Aranovich, G. L.; Donohue, M. D. A New Approach to Analysis of Multilayer Adsorption. *J. Colloid Interface Sci.* **1995**, *173*, 515−520.
(22) Stull, D. R. Vapor Pressure of Pure Substances. Organic and Inorganic Compounds. *Ind. Eng. Chem.* **1947**, *39*, 517−540.
(23) Sips, R. On the Structure of a Catalyst Surface. *J. Chem. Phys.* **1948**, *16*, 490−495.
(24) Toth, J. State Equations of the Solid Gas Interface Layer. *Acta Chim. Acad. Sci. Hung.* **1971**, *69*, 311−317.
(25) Vortmeyer, D.; Adam, W. Steady-State Measurements and Analytical Correlations of Axial Effective Thermal Conductivities in Packed Beds at Low Gas Flow Rates. *Int. J. Heat Mass Transfer* **1984**, *27*, 1465−1472.
(26) Nitta, T.; Shigetomi, T.; Kuro-Oka, M.; Katayama, T. An Adsorption Isotherm of Multi-Site Occupancy Model for Homogeneous Surface. *J. Chem. Eng. Jpn.* **1984**, *17*, 39−45.
(27) Ryu, Y. K.; Lee, S. J.; Kim, J. W.; Leef, C.-H. Adsorption Equilibrium and Kinetics of H2O on Zeolite 13x. *Korean J. Chem. Eng.* **2001**, *18*, 525−530.
(28) Kim, J.-H.; Lee, C.-H.; Kim, W.-S.; Lee, J.-S.; Kim, J.-T.; Suh, J.-K.; Lee, J.-M. Adsorption Equilibria of Water Vapor on Alumina, Zeolite 13X, and a Zeolite X/Activated Carbon Composite. *J. Chem. Eng. Data* **2003**, *48*, 137−141.
(29) Chuikina, V. K.; Kiselev, A. V.; Mineyeva, L. V.; Muttik, G. G. Heats of Adsorption of Water Vapour on NaX and KNaX Zeolites at Different Temperatures. *J. Chem. Soc., Faraday Trans. 1* **1976**, *72*, 1345−1354.
(30) Gopal, R.; Hollebone, B. R.; Langford, C. H.; Shigeishi, R. A. The Rates of Solar Energy Storage and Retrieval in a Zeolite-Water System. *Sol. Energy* **1982**, *28*, 421−424.
(31) Zhu, R.; Han, B.; Lin, M.; Yu, Y. Experimental Investigation on an Adsorption System for Producing Chilled Water. *Int. J. Refrig.* **1992**, *15*, 31−34.
(32) Li, G.; Xiao, P.; Webley, P. A.; Zhang, J.; Singh, R. Competition of CO2/H2O in Adsorption Based CO2 Capture. *Energy Procedia* **2009**, *1*, 1123−1130.
(33) Ferreira, D.; Magalhães, R.; Taveira, P.; Mendes, A. Effective Adsorption Equilibrium Isotherms and Breakthroughs of Water Vapor and Carbon Dioxide on Different Adsorbents. *Ind. Eng. Chem. Res.* **2011**, *50*, 10201−10210.
(34) Chen, D.; Hu, X.; Shi, L.; Cui, Q.; Wang, H.; Yao, H. Synthesis and Characterization of Zeolite X from Lithium Slag. *Appl. Clay Sci.* **2012**, *59* (60), 148−151.
(35) Hefti, M.; Marx, D.; Joss, L.; Mazzotti, M. Adsorption Equilibrium of Binary Mixtures of Carbon Dioxide and Nitrogen on Zeolites ZSM-5 and 13X. *Microporous Mesoporous Mater.* **2015**, *215*, 215−228.
(36) Mette, B.; Kerskes, H.; Drück, H.; Müller-Steinhagen, H. Experimental and Numerical Investigations on the Water Vapor Adsorption Isotherms and Kinetics of Binderless Zeolite 13X. *Int. J. Heat Mass Transfer* **2014**, *71*, 555−561.
(37) Lehmann, C.; Beckert, S.; Nonnen, T.; Gläser, R.; Kolditz, O.; Nagel, T. Water Loading Lift and Heat Storage Density Prediction of Adsorption Heat Storage Systems Using Dubinin-Polanyi Theory—Comparison with Experimental Results. *Appl. Energy* **2017**, *207*, 274−282.
(38) Semprini, S.; Lehmann, C.; Beckert, S.; Kolditz, O.; Gläser, R.; Kerskes, H.; Nagel, T. Numerical Modelling of Water Sorption Isotherms of Zeolite 13XBF Based on Sparse Experimental Data Sets for Heat Storage Applications. *Energy Convers. Manage.* **2017**, *150*, 392−402.
(39) Loughlin, K. F.; Abouelnasr, D.; Mousa, A. al. Saturation Loadings on 13X (Faujasite) Zeolite above and below the Critical Conditions. Part IV: Inorganic Multi-Atomic Species, Halocarbons and Oxygenated Hydrocarbons Data Evaluation and Modeling. *Adsorption* **2018**, *24*, 81−94.
(40) Brandani, F. *Development and Application of the Zero Length Column (ZLC) Technique for Measuring Adsorption Equilibria*. dissertation, The University of Maine, 2002.
(41) Do, D. D. *Adsorption Analysis: Equilibria and Kinetics; Series on chemical engineering*; Imperial College Press: London, England, 1998; Vol. 2.

DOI: 10.1021/acs.jced.8b00961
J. Chem. Eng. Data 2019, 64, 1063−1071